an increase in C_{m_u} results in an increase in ω_p and viceversa above the critical value of the derivative. Figure 1 shows the variation for aircraft F in flight condition 3.

The phugoid frequency remains almost invariant with C_{m_α} until it reaches a critical value $M_\alpha = M_u Z_\alpha / Z_u$, when it becomes zero.[4] At the critical value the phugoid frequency diverges with a slope of $-\infty$. When $M_q Z_\alpha / U_1 < M_u Z_\alpha / Z_u$, the divergence occurs earlier at $M_\alpha = M_q Z_\alpha / U_1$, and the slope of the curve suddenly changes to $+\infty$. Figure 1 shows the change for aircraft C in flight condition 2.

The derivative of ω_p with respect to C_{m_q} is given by

$$\frac{\partial \omega_p}{\partial M_q} = \frac{\overbrace{\omega_p}^{(-)} \overbrace{Z_\alpha}}{2\underbrace{(M_\alpha U_1 - M_q Z_\alpha)}_{(-)}}$$

ω_p is thus directly proportional to M_q. From the definition of C_{m_q} (Ref. 1), it follows that ω_p is also directly proportional to C_{m_q}. Figure 1 depicts the variation for aircraft E in flight condition 1.

It has been shown[5] that in the speed range of interest of powered aircraft ω_p is invariant with respect to changes in the forward speed, dispelling the commonly held notion that the phugoid frequency is inversely proportional to the forward speed.

Effect of Aerodynamic Derivatives on the Phugoid Damping

Unlike the frequency equation, the approximation to damping [Eq. (2)] is comparatively more complicated. All derivatives except C_{D_q}, C_{L_q}, and $C_{L_{\dot\alpha}}$ seem to be involved. The numerical simulation shows that the phugoid damping varies substantially only with the derivatives C_{D_u}, C_{m_u}, C_{m_α}, and C_{m_q}.

From Eq. (2)

$$\frac{\partial(2\zeta_p\omega_p)}{\partial X_u} = \frac{g\sin\Theta_1 M_{\dot\alpha} - M_\alpha U_1 + M_q Z_\alpha}{M_\alpha U_1 - M_q Z_\alpha}$$

$$= -1 + \frac{g\sin\Theta_1 M_{\dot\alpha}}{M_\alpha U_1 - M_q Z_\alpha}$$

$$\approx -1$$

because in practice the second term is much smaller than one. From the definition of X_u (Ref. 1), it follows that $2\zeta_p\omega_p$ increases as C_{D_u} increases. Figure 1 shows significant change for aircraft B in flight condition 2.

$$\frac{\partial(2\zeta_p\omega_p)}{\partial M_u} = \frac{U_1(X_\alpha - g)}{M_\alpha U_1 - Z_\alpha M_q} - \frac{gZ_\alpha[U_1(M_{\dot\alpha} + M_q) + Z_\alpha]}{(M_\alpha U_1 - Z_\alpha M_q)^2} \quad (5)$$

The quantity on the right-hand side is sometimes positive and sometimes negative. The numerical simulation indicates that the phugoid damping remains almost invariant with changes in M_u except when M_u approaches the critical value $M_u = (M_\alpha Z_u)/Z_\alpha$. At this value of M_u, $\omega_p = 0$, and the term $2\zeta_p\omega_p$ abruptly becomes zero. When M_u is less than this critical value, there are two real roots to the phugoid.

The numerical simulation shows that $2\zeta_p\omega_p$ is not disturbed by variations in C_{m_α} except at a critical value of C_{m_α} when it behaves violently by abruptly changing its slope to $\pm\infty$. It may be inferred from Eq. (2) that this behavior is caused by the phugoid frequency, which becomes zero at $M_\alpha = (M_u Z_\alpha)/Z_u$ and becomes infinite when $M_\alpha = (M_q Z_\alpha)/U_1$.

Figure 1 shows that when C_{m_q} becomes more and more negative $2\zeta_p\omega_p$ increases in magnitude. The increase is substantial in some cases and mild in others. Figure 1 shows the variation for aircraft E in flight condition 1.

Conclusion

The parametric study undertaken in this paper shows that in the range of interest the frequency and the damping depend only on the derivatives C_{D_u}, C_{m_u}, C_{m_α}, and on C_{m_q}. The speed damping derivative C_{D_u} has no effect on the frequency. The damping increases with increase in C_{D_u}. Phugoid damping is invariant with change in C_{m_u}. When $M_u = (M_\alpha Z_u)/Z_\alpha$, the phugoid frequency vanishes. For M_u less than this critical value, the phugoid mode splits into two first-order roots, with one representing tuck under. Above the critical value, increase of C_{m_u} leads to increase in ω_p. The phugoid damping is invariant with change in C_{m_α}. For large negative values of C_{m_α}, ω_p remains invariant. When $M_\alpha = (M_u Z_\alpha)/Z_u$, the phugoid frequency vanishes. When $M_\alpha = (M_q Z_\alpha / U_1)$, the phugoid frequency becomes infinite. Increase in $|C_{m_q}|$ results in decrease in ω_p (for negative values of C_{m_q}), and increase in $|C_{m_q}|$ results in increase in $2\zeta_p\omega_p$ (for negative values of C_{m_q}). The change is substantial in some cases and mild in others.

Acknowledgment

The author is grateful to the Aeronautics Research and Development Board, New Delhi, India, for providing financial support for this research.

References

[1]Roskam, J., "Airplane Flight Dynamics and Automatic Flight Controls," DAR Corp. Pt. I, Lawrence, KS, 1998.

[2]Kamesh, S., and Pradeep, S., "The Phugoid Approximation Revisited," *Journal of Aircraft*, Vol. 36, No. 2, 1999, pp. 465–467.

[3]Pradeep, S., "A Century of Phugoid Approximations," *Aircraft Design*, Vol. 1, No. 2, Elsevier, Oxford, England, UK, 1998, pp. 89–104.

[4]Pradeep, S., "A Note on the Aft C. G. Location," AIAA Paper 2000-4114, Aug. 2000.

[5]Pradeep, S., and Kamesh, S., "Does the Phugoid Frequency Depend on Speed?" *Journal of Guidance, Control, and Dynamics*, Vol. 22, No. 2, 1999, pp. 372, 373.

Wave Drag Estimation for Use with Panel Codes

N. Petruzzelli* and A. J. Keane†
University of Southampton, Highfield, Southampton, England SO17 1BJ, United Kingdom

I. Introduction

FOR transonic wing designs one of the most important elements in the analysis of aerodynamic performance is the evaluation of wave drag. A common technique for estimating the wave drag of a wing consists in summing the contributions at spanwise sections over the wing. The contribution at each section may be evaluated using methods derived from an exact two-dimensional analysis involving the flow conditions just upstream of the shock wave.[1,2] For each section of the wing, the equivalent two-dimensional flow conditions are then evaluated from the three-dimensional flow conditions using simple sweep theory. The major drawback of such a method is the need for data coming from the three-dimensional flow state around the wing through experimental measurements or full three-dimensional compressible flow state calculations. Such an approach turns out to be not very useful in the context of preliminary concept design, where expensive three-dimensional compressible flow evaluations are to be avoided, where possible, during design optimization. Thus, to reduce the computational cost of wing wave drag evaluation in preliminary design, approximate methods that do not require expensive three-dimensional flow state calculations may be adopted.

Received 19 October 2000; revision received 22 February 2001; accepted for publication 27 February 2001.

*Research Fellow, School of Engineering Sciences. Member AIAA.

†Professor of Computational Engineering, School of Engineering Sciences.

In Ref. 3, Van der Velden et al. propose a method that predicts he minimal achievable transonic drag as a function of wing pre-iminary design parameters. The method is based on a database of irfoils designed for minimum drag under representative specific op-rating and geometric constraints. For a given planform, thickness, nd load distribution, the equivalent two-dimensional flow condi-ions on a straight tapered section of the wing are determined using he sweep angle of the shock. Because the location of the shock on ne chord for each airfoil in the database is known, the shock sweep an be determined iteratively for each combination of section and irfoil. The two-dimensional airfoil drag of the wing section is then ecovered from the database and converted into the correspond-ig three-dimensional value using a modified version of Boppe's weep–taper theory[4] and the value of the shock sweep. The local ave drag values can then be integrated along the span leading to ie overall wave drag of the wing.

The described approach is based on the observation that, though ansonic wings are designed with respect to many operating points, e wave drag at the principal cruise operating point is very close the minimal achievable wave drag. This is valid in practice for bsonic long-range transports because they spend most of their time the cruise operating condition, but it may not be so applicable r other transport ranges. Moreover, such a hypothesis prevents ideoffs of the various components of drag from being investigated. nother restriction of this approach is the assumption that during eliminary design the wing will be described in terms of planform d thickness distribution, and the detailed shapes of the individual ctions of the wing will not be available. This means that wave drag n not be evaluated directly because it depends on the curvature of wing sections, and approximate methods have also to be used for prediction of the spanwise loading. Such an approach is common many concept design tools and, although it has the advantage of needing to call on sophisticated computational fluid dynamics FD) codes, runs the risk of limiting improvements in design, even nly the overall planform and other major parameters are being estigated.

n Ref. 5, Robinson and Keane describe an approach to section deling, where each section is described as a linear combination a set of orthogonal shape functions derived from a series of a ercritical transonic two-dimensional aerofoil sections. Such or-gonal shape functions can be used to construct those foils in original set of airfoils, when combined together in appropriate os, or other related section shapes by using other mixes. The posed method allows for up to six such base shapes to be used his process, but demonstrates that the shapes and aerodynamic ormance of the original airfoils can be recovered to reasonable cision with just two functions, which essentially reflect thickness hord ratio and camber.

he ability to represent an airfoil with just two base function-ghting parameters offers the possibility of defining an effective efficient geometric model of the wing sections, well suited to preliminary design stage. Following this approach, once the kness to chord ratio, twist, and camber distributions along the g are known, the full shape of the wing may be defined for equent analysis by CFD codes (or any other form of analysis). allows for more accurate design performance estimations and off studies to be carried out between the different components ag. In this work, an approximate method for the estimation of vave drag of transonic wings described in this way is presented. aim is to devise an efficient wave drag estimation method for with panel codes that is especially suitable for the preliminary design process.

ie work described here uses the airfoil representation for wing on parameterization of Robinson and Keane.[5] The aim is to iate the wave drag of a three-dimensional wing just using data ng from accurate two-dimensional flow analyses. The desire is aluate the contribution of each section of the wing to the over-ave drag by reconstructing an equivalent two-dimensional flow icterized by the same local wave drag value. To define how such uivalent two-dimensional flow might be reconstructed, com-ible two-dimensional flow analyses of several profiles derived from transonic wing sections have been performed. Mach number distributions around the two-dimensional profiles have then been compared to those around the complete three-dimensional wing to understand under what geometric and flow state conditions the wave drag values match. This study is described in Sec. II. Then, in Sec. III, an equivalence between the three-dimensional and two-dimensional wave drag values is derived based on the application of simple sweep concepts and equivalent camber distributions of the local spanwise wing sections. Finally, in Sec. IV, the method is applied to computation of the wave drag of a transonic wing and a comparison made with a more accurate evaluation based on data coming from a full compressible three-dimensional flow analysis.

II. Three-Dimensional and Two-Dimensional Wave Drag Evaluations

Consider an aircraft wing at a Reynolds number of 7.3×10^6, Mach number of 0.785, and angle of attack of 1.52 deg. The wing geometry data are given in Table 1.

The envelope of the wing has been constructed using 18 sections uniformly distributed along the wing span, as shown in Fig. 1. Each section has been defined as a linear combination of two orthogonal functions, according to the strategy described in Ref. 5. These functions represent the t/c distribution and the camber of the section. Once the spanwise distribution of these functions along the wing is known, the full geometric description of the wing may be constructed for subsequent analysis by the CFD codes. In this case, the thickness to chord ratio distribution is input, whereas the camber distribution is found by prescribing a spanwise lift distribution that minimizes the sum of wave and induced drag, also following the approach outlined in Ref. 5. A full three-dimensional flow state evaluation has been performed for this design using the MGAERO three-dimensional Euler solver[6] followed by application of Lock's second-order method[1] (also known as the Engineering Sciences Data Unit method[2]) to provide a wave drag estimate from the resulting flow information. This wave drag estimation uses relations based on the Mach number immediately upstream of the shock

Table 1 Wing geometry data

Quantity	Value
Wing area, m^2	168
Aspect ratio	9.07
Kink position (fraction of span)	0.313
Sweep angle, deg	27.1
Inboard taper ratio	0.6
Outboard taper ratio	0.51
Root t/c	0.15
Kink t/c	0.122
Tip t/c	0.122
Wash out at tip, deg	4

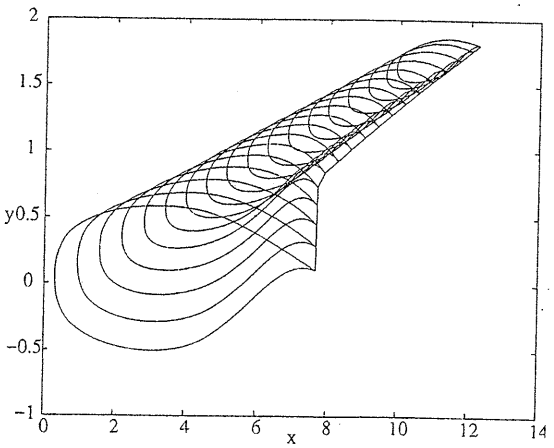

Fig. 1 Wing sections.

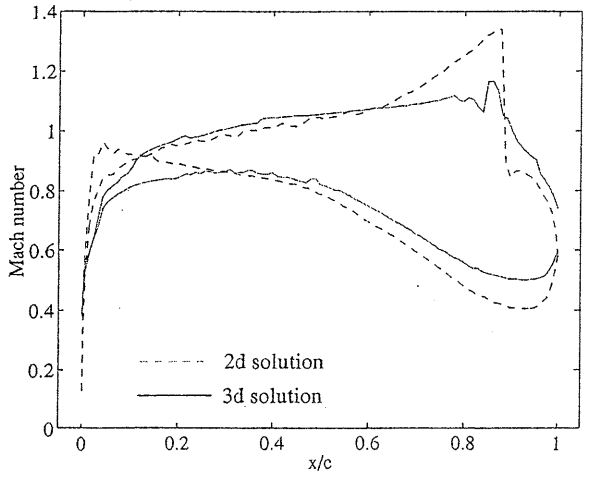

Fig. 2 Case 1, Mach number distributions over the equivalent two-dimensional section and wing section.

together with the mean aerofoil surface curvature over the region upstream of the shock. The three-dimensional code also provides a complete set of output flow variables values for each section of the wing.

First, consider a section of the wing located at 37% span. This section is characterized by a t/c value of 0.122, a camber weighting parameter β of -0.160, and an angle of attack of -0.069 deg (downwash angle included). The solid line in Fig. 2 represents the Mach number distribution over the section taken from the three-dimensional Euler solution (case 1). Here the supersonic region over the upper surface ends near the trailing edge through a weak shock. In this case the wave drag is almost negligible, its value being only 0.45 counts. In an attempt to find an equivalent two-dimensional flow, consider a section with equivalent effective values of t/c, Cl, and flow conditions characterized by effective Mach number, that is, from simple sweep theory. In this first case, the same camber as that for the three-dimensional wing section has been used. The two-dimensional flow solution has been computed with the two-dimensional MGAERO solver, using its internal angle-of-attack control feature to provide the desired section lift coefficient. The dashed line in Fig. 2 represents the corresponding Mach number distribution. A well-defined shock wave can be identified on the upper surface of the equivalent section for the two-dimensional analysis, corresponding to a value of the wave drag of 29 counts. The resulting value of the angle of attack is -2.69 deg, far from its value in the three-dimensional flow of -0.07 deg. Clearly, the two-dimensional section is not a good match for the three-dimensional flow.

Next a case has been considered where the camber value is allowed to change to find a two-dimensional flow characterized by the same wave drag value as the flow over the three-dimensional wing section. To achieve this the camber weighting function value β has been varied from -0.15 to 0.10 (case 2). The value of the camber function weight for which the two-dimensional flow best matches the three-dimensional wave drag value is approximately -0.08, with an angle of attack of -1.54 deg. For higher or lower values of the camber function, well-defined shock waves appear on the upper surface of the section (near the trailing edge for low β/high camber and the one-third chord point for high β/low camber). Figure 3 shows the two-dimensional matching Mach number distribution (dashed line) compared with the three-dimensional distribution. The variation of camber allows for a choice of a section with the same wave drag as the section of the three-dimensional wing, the angle of attack being somewhat different from its value in the three-dimensional flow. Table 2 summarizes the matching case.

Next, the sweep angle of the wing is changed from the preceding value of 27 deg to a value of 20 deg, while conserving the total lift coefficient (case 3). The three-dimensional MGAERO solution then gives an angle of attack of 0.90 deg. The section located at near

Table 2 Case 2 data

Quantity	Wing section (three-dimensional)	Matching section (two-dimensional)
Mach number	0.785	0.718
t/c	0.122	0.133
Cl	0.5968	0.7133
Camber function value	−0.160	−0.08
Angle of attack, deg	−0.069	−1.538
Wave drag (counts)	0.45	0.47

Table 3 Case 4 data

Quantity	Wing section	Matching section
Mach number	0.785	0.753
t/c	0.122	0.127
Cl	0.603	0.657
Camber function value	−0.159	−0.047
Angle of attack, deg	−0.50	−1.14
Wave drag (counts)	19.8	20.5

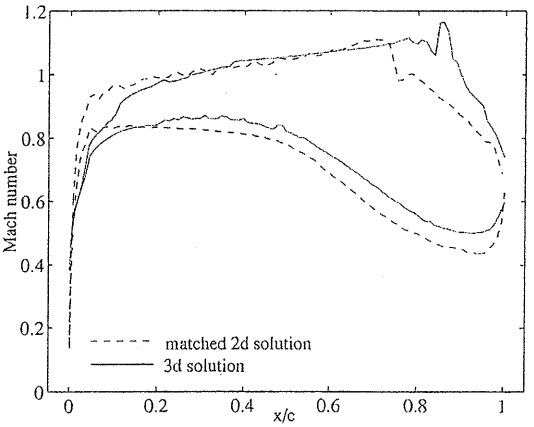

Fig. 3 Case 2, Mach number distribution over the matched two-dimensional section and wing section.

midspan has been considered. The angle of attack of this section is equivalent to -0.22 deg. Figure 4 shows the Mach number distributions of the wing section obtained from the three-dimensional flow solution (solid line) together with that obtained from the two-dimensional flow solution with identical camber (case 3, dashed line). This time a better-defined shock wave appears in the three-dimensional solution as its strength grows with decreases in sweep angle of the wing ($M > 1.2$), despite the reduced value of the angle of attack. In fact, the local three-dimensional wave drag value is 19.3 counts, whereas the two-dimensional solution produces an even stronger shock with a wave drag of 80.9 counts. A similar study as in the preceding case has then been conducted by varying the camber function for the two-dimensional section in the range -0.16–0.01 (case 4). The three-dimensional wave drag is matched for a value of the camber function of approximately -0.047 and an angle of attack of -1.14 deg. The matching Mach distribution is also reported in Fig. 4 (symbols). Table 3 summarizes the data for this case.

III. Geometric Equivalence

Table 4 gives the values of the two-dimensional flow angle of attack obtained when varying the camber weight function values β in the range considered in each of the preceding cases together with the corresponding three-dimensional flow values. It appears, from an analysis of these data that the value of β for the two-dimensional section for which the two-dimensional and three-dimensional wave drag values best match, β_{2d}, is a weighted sum:

$$\beta_{2d} = (3\beta_{\alpha 2d=\alpha 3d} + \beta_{3d})/2 \qquad (1)$$

Table 4 Cases 3 and 4 angles of attack and camber weighting functions

Quantity	Three-dimensional	Two-dimensional						
				Case 3				
α	−0.069	−2.438	−2.014	−1.538	−1.366	−0.991	−0.116	0.603	1.268
β	−0.16	−0.15	−0.11	−0.08	−0.07	−0.05	0.00	0.05	0.10
				Case 4				
α	−0.219	−2.781	−2.668	−2.23	−2.306	−1.141	−1.132	−0.605	−0.427
β	−0.16	−0.160	−0.149	−0.115	−0.103	−0.047	−0.035	−0.001	0.010

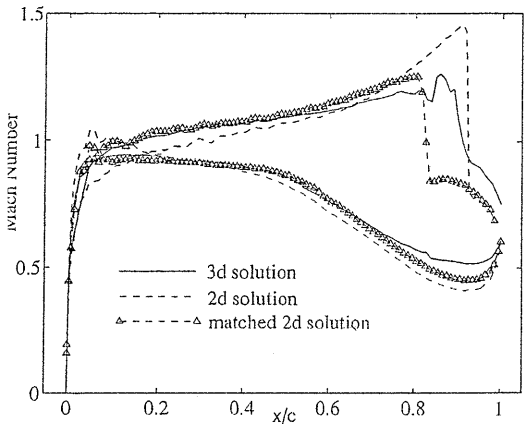

Case 3, Mach number distributions over the equivalent two-
ional section, matched two-dimensional section, and wing sec-

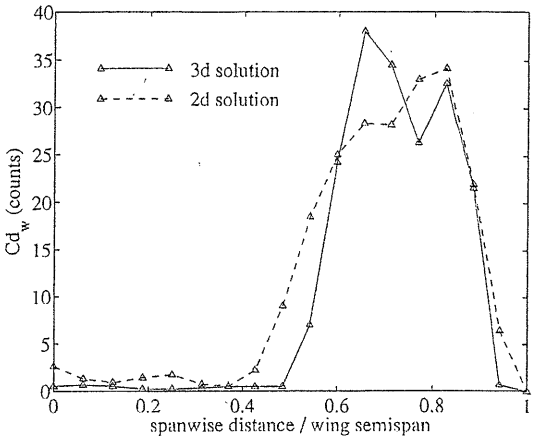

Fig. 5 Local C_{Dw}.

$\beta_{(\alpha 2d=\alpha 3d)}$ is the value of β for which the angles of attack and β_{3d} is that of the wing section. For cases 2 and 4 this a produces, respectively,

$$\beta_{2d} = (3 \times 0.006 - 0.16)/2 = -0.071 \tag{2}$$

$$\beta_{2d} = (3 \times 0.023 - 0.16)/2 = -0.046 \tag{3}$$

values should be compared with those of −0.08 and −0.047 l earlier for these two cases.

Estimation of Wave Drag for a Transonic Wing

lustrate this process, the results described in the preceding are next applied to the estimation of wave drag for the com- nsonic wing having the parameters already noted in Table 1.) automate the search for equivalent two-dimensional flows, of flow analyses of two-dimensional profiles of unit chord have been performed with the two-dimensional version of AERO solver. A range of different flow conditions and t/c tions have been considered corresponding, respectively, to of Mach number of 0.7, 0.75, 0.78, and 0.8 and t/c ratios of).1, 0.125, and 0.15, while allowing the camber weighting to d in the range −0.5–0.6 in 12 steps, and Cl in the range 0–0.8 ps. For each of these combinations, the value of the angle of s recovered (using the internal angle of attack control feature AERO to provide the given lift coefficient), together with the f wave drag (using Lock's[1] second-order method). Having ich a two-dimensional database, a look-up table approach is ed to find the equivalent three-dimensional wave drag. This h enables the value of β that matches the three-dimensional ction angle of attack to be found by interpolation for given , and Mach number and then the value of wave drag coeffi- gain by interpolation, once the equivalent camber function has been derived from Eq. (1). The wave drag coefficient is, mputed on a basis of flow conditions and geometric quanti- ving from two-dimensional equivalence considerations, that is, from sweep theory, using two-dimensional profiles of unit chord length. The local wave drag coefficient C_{Dw} of the three-dimensional wing is then given by

$$C_{Dw} = C^*_{Dw} \cos^3 \Lambda / c \tag{4}$$

where C^*_{Dw} is the wave drag coefficient of the matched two-dimensional profile, Λ is the sweep angle of the shock on the upper surface of the wing (here taken parallel to the outboard trailing edge), and c is the local chord length. The local wave drag coefficients can then be integrated along the span leading to the overall wave drag coefficient of the wing. Figure 5 shows the local wave drag coefficients as computed by this approximate method (dashed line) compared with those from using the flow data values of a full three-dimensional analysis (solid line).

The approximate C_{Dw} of each section has been computed using the local Cl and angle of attack of a three-dimensional flow solution produced using a panel code.[7] Moreover, the local angles of attack have been defined by taking into account the local twist and a downwash angle simply computed from an elliptic spanwise lift distribution.

Notice that the drag coefficient is underestimated in the middle of the semispan and slightly overestimated toward the root and the tip. The overall drag coefficient predicted by the approximate method is 9.7 counts, just 1.7 counts higher than the accurate value from the full three-dimensional solution.

The entire procedure for the wing wave drag evaluation can thus be summarized as follows:

1) Solve the flow for the wing configuration under consideration using a noncompressible flow solver (panel code) and recover the spanwise loading distribution and the angle of attack.

2) For each spanwise wing section a) compute Mach_{2d}, Cl_{2d}, and t/c_{2d}, using the sweep angle of the shock (assumed parallel to the outboard trailing edge); b) compute the angle of attack α_{3d} using the section twist and a downwash angle based on the equivalent elliptic spanwise loading distribution (a better estimate of the section downwash angle may be made using a sine series decomposition of the actual loading distribution[8]); c) pick up $\beta_{(\alpha 2d=\alpha 3d)}$ from the look-up table using t/c_{2d}, Mach_{2d}, Cl_{2d}, and α_{3d} as input data; and

Table 5 Drag coefficients values

Mach no.	Sweep angle, deg	Euler drag (counts)			Panel drag (counts)		
		C_{Dw}	Cd	$(C_{Dw}/Cd)\%$	C_{Dw}	Cd	$(C_{Dw}/Cd)\%$
0.785	25	15.0	177.0	8.7	17.1	188.7	9.1
0.785	27.1	8.0	171.4	4.7	9.7	176.4	5.5
0.8	30	16.7	175.6	9.5	15.1	181.7	8.3
0.8	35	7.6	165.9	4.6	8.7	172.7	5.1
0.85	30	26.1	175.9	14.8	25.7	159.4	16.2
0.85	35	3.5	147.6	2.4	4.8	152.8	3.1
0.9	35	29.7	151.5	19.6	23.9	147.4	16.2

d) compute β_{2d} from Eq. (1) and then pick up C_{Dw} from the look-up table using t/c_{2d}, Mach_{2d}, Cl_{2d}, and β_{2d} as input data.

3) Integrate the wing section wave drag coefficients along the span for the overall wave drag coefficient of the wing.

It seems that despite the various approximations involved in the evaluation of the local angles of attack, this approach does not prejudice the prediction of the wave drag via two-dimensional values. Numerical experience has shown that a variation in the angle of attack up to 1 deg gives errors in the wave drag values of just a few counts.

Wave drag values computations for different wing configurations over a wide range of geometries have confirmed that the agreement between the Euler-based method and the Panel-based method of estimation is maintained over a range of Mach numbers. Table 5 gives values of the wave drag and the overall drag for Mach number and sweep angle varying, respectively, from 0.785 to 0.9 and from 25 to 35 deg, as predicted by the two methods. As may be seen, the difference between the wave drag values lies in the range 0.4–2.0 counts, except for the case with Mach number of 0.9 and sweep angle of 35 deg, where the difference rises to 5.9 counts. It is clear that, at such sweep and Mach number, flow conditions are highly three dimensional and that the drag estimates of the panel-code-based method are beginning to be misleading. Nevertheless, in all of the cases, the relative wave drag values of the two methods with respect the corresponding overall drag values differ by no more than 3.4%.

In Ref. 9, the method described in this paper has been integrated into a multilevel optimization methodology for the preliminary concept design of transonic wings. The methodology was mainly characterized by the use of different flow analysis levels, ranging from an empirical model through a linearized potential method to an Euler method. The utility of the method has been twofold. First, the method has supplied a reliable wave prediction capability to the linearized potential code. Second, the method has been employed as a design tool for defining a camber variation along the wing that may be used to minimize the sum of induced and wave drag. When used in this fashion, the method allows for tradeoffs of induced and wave drag without calling either of the CFD codes. More precisely, the wave drag is evaluated using a lift distribution based on the camber data and an angle of attack based on an estimated lift curve, whereas the induced drag is found by simply integrating the lift. Numerical results demonstrate the ability of such an approach to lead to good wing shape designs, thus demonstrating the effectiveness and robustness of the proposed method for evaluating the wave drag of transonic wings.

V. Conclusion

A new method for estimating the wave drag of swept three-dimensional wings in transonic flows has been described. This may be used in conjunction with panel codes during concept design studies. Using simple sweep theory and information on the wing shape, the method evaluates the contribution of each spanwise wing section to the overall wave drag by reconstructing an equivalent two-dimensional flow characterized by the same local wave drag value. Then a routine applying data derived from the offline analysis of all of the possible two-dimensional sections in use (by an Euler code) estimates the wing wave drag. This makes use of spanwise loading distribution and angle of attack calculated by the panel code or from suitable approximations. The effectiveness of the method has been assessed by comparison with a more accurate wave drag evaluation method based on data coming from full three-dimensional compressible flow analyses. The differences between these approaches have been shown to be in the range of just a few drag counts.

Aimed at providing a reliable wave prediction capability to linearized potential codes, the method is especially suitable for the preliminary concept wing design process, where analyses based on expensive three-dimensional compressible flow evaluations are avoided if at all possible. Moreover, because curvature information of the wing sections is taken into account, the method allows tradeoff studies of the various drag components to be carried out, thus enabling sophisticated definition of the wing shape in the early stages of the design process.

No doubt the approach proposed would not work so well at higher speeds or extreme sweep angles when only a full, compressible three-dimensional analysis can accurately describe the flow conditions.

Acknowledgments

The work described in this paper was supported by the Engineering and Physical Sciences Research Council of the United Kingdom under Grant Reference GR/L04733 and also by BAE Systems.

References

[1]Lock, R. C., "Prediction of the Drag of Aerofoils and Wings at High Subsonic Speeds," *Aeronautical Journal*, Vol. 90, No. 896, 1986, pp. 207–226.

[2]"A Method for Determining the Wave Drag and Its Spanwise Distribution on a Finite Wing in Transonic Flow," ESDU 87003, Engineering Sciences Data Unit, London, 1987.

[3]Van der Velden, A., Kelm, R., Kokan, D., and Mertens, J., "Application of MDO to Large Subsonic Transport Aircraft," AIAA Paper 2000-0844, 2000.

[4]Boppe, C., "X-29 Aerodynamic Design and Performance," *Aerodynamic Analysis and Design*, AIAA, Reston, VA, 1988.

[5]Robinson, G. M., and Keane, A. J., "A Case for Multi-level Optimization in Aeronautical Design," *Aeronautical Journal*, Vol 103, 1999, pp. 481–485.

[6]Epstein, B., Luntz, A., and Nachson, A., "Multigrid Euler Solver About Aircraft Configurations, with Cartesian Grids and Local Refinement," AIAA Paper 89-1960, 1989.

[7]Maskew, B., "Prediction of Subsonic Aerodynamic Characteristics: A Case for Low-Order Panel Methods," *Journal of Aircraft*, Vol. 19, No. 2, 1982, pp. 157–163.

[8]Stinton, D., *The Anatomy of the Aeroplane*, Blackwell Science, Oxford, U.K., 1999.

[9]Keane, A. J., and Petruzzelli N., "Aircraft Wing Design Using GA-based Multi-level Strategies," AIAA Paper 2000-4937, Sept. 2000.